

Research

DECOVALEX III PROJECT

Thermal-Mechanical Modeling of the Yucca Mountain Project Drift Scale Test

Task 2B/2C Final Report

Compiled by:
Robin N. Datta

February 2005

With contributions from:
Sebastia Olivella
Claudia Gonzalez
Antonio Gens
Alain Millard
Jonny Rutqvist
Sui-Min Hsiung
Asadul H. Chowdhury

Research

DECOVALEX III PROJECT

Thermal-Mechanical Modeling of the Yucca Mountain Project Drift Scale Test

Task 2B/2C Final Report

Compiled by:
Robin N. Datta

Bechtel SAIC Company, Las Vegas, USA

February 2005

With contributions from:

Sebastia Olivella¹

Claudia Gonzalez¹

Antonio Gens¹

Alain Millard²

Jonny Rutqvist³

Sui-Min Hsiung⁴

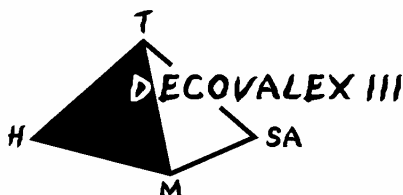
Asadul H. Chowdhury⁴

¹University Polytechnique of Catalina, Barcelona, Spain

²CEN Saclay, Paris, France

³Lawrence Berkeley National Laboratory, Berkeley, California, USA

⁴Center for Nuclear Waste Regulatory Analysis, San Antonio, Texas, USA



SKi

This report concerns a study which has been conducted for the DECOVALEX III Project. The conclusions and viewpoints presented in the report are those of the author/authors and do not necessarily coincide with those of the SKI.

1. Yucca Mountain Project Drift Scale Test

1.1 Yucca Mountain Project Drift Scale Test

The DST in Yucca Mountain in Nevada, USA is a large scale, long term field thermal test being conducted for the U.S. DOE. In the DST a ~5 m diameter drift, ~ 50 m long is being heated by electrical heaters to study the response of the surrounding rock mass to the heating and subsequent cooling. The test is an integral part of DOE's program of site characterization at Yucca Mountain to assess whether the mountain is suitable site for a repository for the disposal of high level nuclear waste and spent nuclear fuel. In Task 2 of DECOVALEX III project the DST is a test case in the process of developing and validating coupled process models. Before the heating phase of the DST at Yucca Mountain was started in December 1997 modeling of various coupled processes was carried out to predict the measurements to be made in the test. These pre-test simulations were performed by U.S. DOE sponsored research teams at the national laboratories. Subsequently, Task 2 participants of DECOVALEX III project independently performed predictive modeling of the DST.

In the broadest sense the primary purpose of the DST is to develop a thorough understanding of the coupled thermal (T), mechanical (M), hydrologic (H), and chemical (C) processes in the rock mass immediately surrounding the proposed repository because of the decay heat from the nuclear waste. To achieve this primary purpose a series specific sub-tier test objectives are established, categorized around the four principal processes of concern. These test objectives are:

Thermal

- ☐ Measure the temporal and spatial distributions of temperature
- ☐ Evaluate influence of heat transfer modes
- ☐ Investigate possible formation of heat pipes
- ☐ Determine rock mass thermal properties

Mechanical

- ☐ Measure rock mass mechanical properties
- ☐ Evaluate ground support response under controlled conditions
- ☐ Measure drift convergence at elevated temperatures
- ☐ Observe effect of thermal loading on prototypical ground support systems and overall room stability

Hydrological

- ☐ Measure changes in rock saturation
- ☐ Monitor the propagation of drying and subsequent re-wetting, if any, including potential condensate cap and drainage
- ☐ Measure changes in bulk-permeability (pneumatic)
- ☐ Measure drift-air humidity, temperature, and pressure

Chemical

- ☐ Collect and analyze samples of water and gas

- ❑ Analyze changes in typical waste package material left in the heated drift
- ❑ Observe changes in water and mineral chemistry from drying and reflux conditions

1.2 Test setting and test facility

A description of the setting of the DST and the test facility can be found in Datta et al.(1999) which is the basis of the following descriptions.

Yucca Mountain, approximately 135 kilometers northwest of Las Vegas, Nevada is part of a series of north-trending ridges in the Great Basin physiographic province of North America. The mountain is underlain by 1000 to 1500 meters of Tertiary volcanic tuffs, formed from the ash of eruptions occurring between 8 and 16 million years ago. The volcanic tuffs are generally bedded, separated in beds that are generally non-welded to densely welded, and in addition, some are devitrified and others are vitric. The proposed repository horizon is within a sequence of beds, up to 350 meters thick, of moderately to densely welded devitrified tuff known as the Topopah Spring Tuff of the Paintbrush Group. The sub-units of the Topopah Spring Tuff are based primarily on the abundance of lithophysae which are cavities with dimensions on the order of millimeters to hundreds of millimeters, formed due to the presence of gases in the cooling ash flows. The presence or absence of lithophysae can have a pronounced effect on the mechanical and hydrologic properties of the rocks.

Topopah Spring Tuff is divided into four sub-units: the upper and lower lithophysal and the middle and lower non-lithophysal. The geologic symbols for the upper and lower lithophysal sub-units are Tptpul and Tptpll respectively while those for the middle and lower non-lithophysal sub-units are Tptpmn and Tptpln respectively. The lower non-lithophysal sub-unit (Tptpln) is stratigraphically the lower most, overlain by Tptpll, Tptpmn, and Tptpul in that order. The bulk of the proposed repository will be located in the lower lithophysal (Tptpll) sub-unit, with small portions in the middle and lower non-lithophysal sub-units. In the hydrologic stratigraphy of the Yucca Mountain area, the symbols for these sub-units of Topopah Spring Tuff are tsw33, tsw34, tsw35, and tsw36 with tsw36 being the lower most and tsw33 being the upper-most, corresponding to Tptpln and Tptpul respectively.

The DST is located entirely in the middle non-lithophysal sub-unit of Topopah Spring Tuff represented by Tptpmn or tsw34. These geologic or hydrologic symbols are frequently employed in this report to specify the beds.

The DST consists of a 47.5m long, 5m diameter drift heated by nine canister heaters, each 1.7m diameter, 4.6m long, placed on the floor of the drift. Additional heat is supplied by 50 rod heaters, referred to as “wing heaters” inserted into horizontal boreholes drilled into each sidewall. (Figure 1.1). The drift cross-section and the canister heaters are approximately the sizes of drifts and waste packages, respectively, being currently considered for the potential repository. The wing heaters are used to simulate the heat that would come from adjacent drifts in a repository, and thus provide better test boundary conditions. Each canister heater can generate a maximum of 15kW. The wing heaters are each 10 meters long, and have inner and outer segments that can generate 1145W and 1719W, respectively. Rockbolts and wire-meshes are installed as ground support along the entire length of the Heated Drift. In addition, the final 12.5m length of the drift was supported by a cast-in-place concrete liner to observe the performance of a concrete-lined drift at elevated temperatures. An access/observation drift excavated parallel to the heated drift, and a perpendicular connecting drift are

constructed around the periphery of the test block (Figure 1.1). The heated length of the drift is isolated from the connecting drift by an insulated thermal bulkhead. The bulkhead is not a pressure bulkhead. This means that some heat exchange by convection through the bulkhead will occur. Approximately 3300 meters of boreholes are drilled from the heated drift, the connecting drift and the access/observation Drift into the test block (Figures 1.1 and 1.2) to house the wing heaters and approximately 3500 sensors of various types. By the end of the heating phase of the test extending over four years, approximately 15,000 m³ of rock will be heated above 100 degree Celcius. For complete and full descriptions of the DST, refer to the reports, “Drift Scale Test Design and Forecast Results” (CRWMS M&O, 1997) and “Drift Scale Test As-Built Report” (CRWMS M&O, 1998).

1.3 Measurements dada

The following measurements are being made or were planned to be made in the DST:

1. Heater Power
2. Rock temperature by thermocouples and resistance temperature devices
3. Displacement in rock by multiple borehole extensometers
4. Deformation of concrete lining by convergence monitors
5. Strain in concrete by strain gages
6. Moisture content of the rock by neutron logging
7. Moisture content of the rock by electric resistivity tomography (ERT)
8. Moisture content of the rock by ground penetrating radar (GPR)
9. Acoustic or microseismic emissions
10. Relative humidity, temperature, and air pressure in sections of boreholes isolated by packers
11. Relative humidity, temperature, and air pressure in the Heated Drift and outside
12. Changes in fracture permeability (k) by pneumatic methods (air permeability) and gas tracer tests
13. Analyses of gas and water samples collected from the test block
14. Thermal conductivity and diffusivity by REKA (rapid evaluation of K and alpha) probe
15. Periodic video and infrared images of the inside of the Heated Drift
16. Rock mass modulus of deformation by the plate-loading test
17. Temperature on non-rock surfaces such as heaters, bulkhead, cable-trays, etc. using thermocouples
18. Mineralogic-petrologic characteristics of the rock before and after the test
19. Thermal, mechanical, and hydrologic properties of intact rock samples measured in the laboratory, before and after the test

In addition to the above, coupons of candidate materials for the waste container, cylindrical samples of concrete used for the cast-in-place liner, and native microbes have either been left in the Heated Drift or injected into the test block to study the effects of prolonged heating and cooling on them.

An approximately 6000 channel, automated data collection system (DCS) records measurements on an hourly basis. The DCS scans and records the readings of temperature, humidity, air pressure, MPBXs, strain gages, convergence monitors, and current and voltage for heater power. Other measurements, referred to as active testing, such as air-K measurements, neutron logging, ERT, acoustic emission, GPR, and

REKA probe measurements are recorded periodically using independent data acquisition systems.

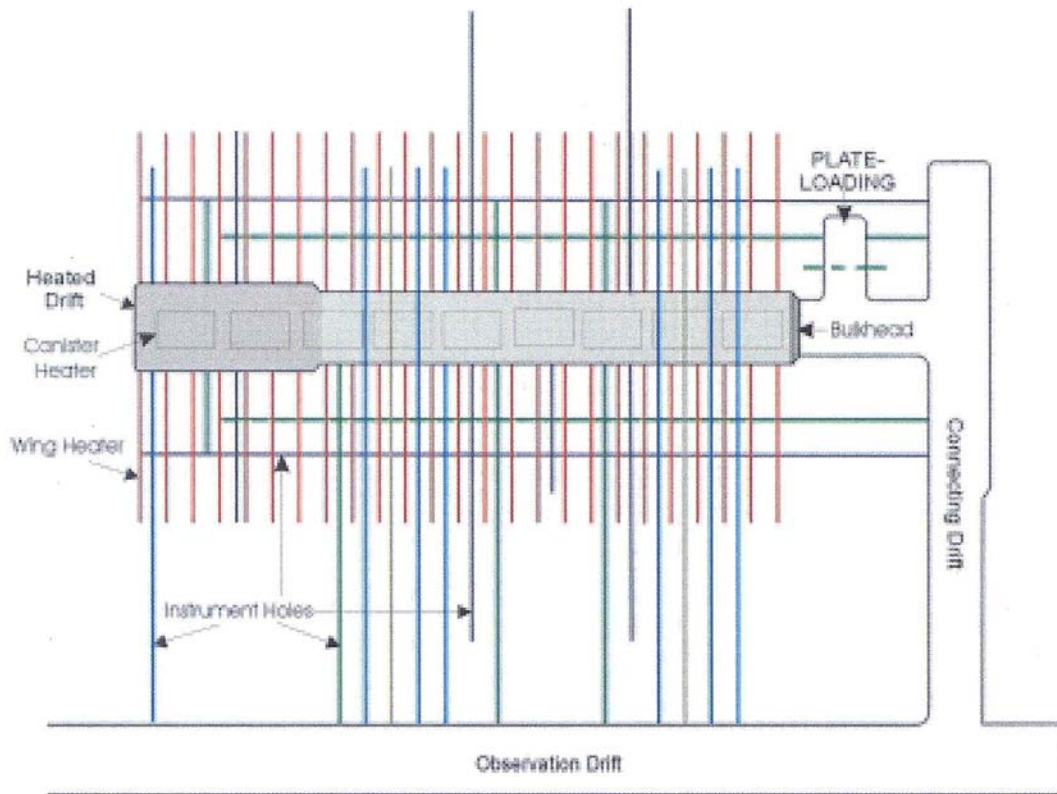


Figure 1.1. Location of the wing heaters, canister heaters and instrument holes in the Drift Scale Test.

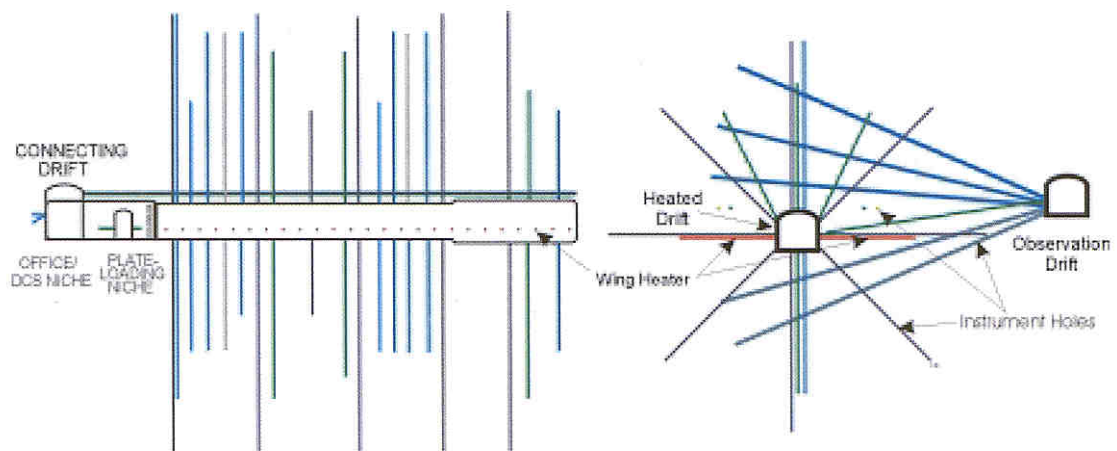


Figure 1.2. a) Cross-section parallel to the heated drift; b) Cross-section orthogonal to the heated drift.

2. Task 2B/2C – Thermo-mechanical simulation

Task 2 of the DECOVALEX III project is centered around the DST. There are four sub-tasks in Task 2 to study the heat-driven coupled processes of interest. Task 2A is to study the TH response of the test block, while 2B/2C and 2D are to study the THM/TM and THC responses respectively.

2.1 Task 2B/2C definition

Tasks 2B and 2C deal with the mechanical process in the DST during the heating and cooling phases of the test. To model mechanical processes in the test it is necessary to have the time-evolution of temperature distributions in the test block which are inputs in the calculation of the mechanical effects. The difference between task 2B and 2C is that in 2B the mechanical effects are simulated using modeled temperature distributions as inputs, while in 2C the mechanical effects are calculated using measured temperature distributions as inputs. Otherwise, tasks 2B and 2C are defined as follows:

Given

- a) Results of geologic, thermal, mechanical, hydrologic, and mineralogic/petrologic characterization of the test block of the DST
- b) As-built configuration of the test block, including locations of various sensors and measuring instruments
- c) Plans of heating and cooling, including expected heater powers at various times

Tasks:

Predict the time-evolution of the displacements in the test block measured in the MPBX holes; a suitable time Interval such as 10, 30, 50, or 100 days may be used
Predict the changes in the (fracture) permeability of the rock due to thermal-mechanical processes; a time interval of 10,30, 50, or 100 days may be used.

2.2 The Task 2B/2C research teams

Besides the U.S. DOE's Office of Repository Development (ORD) formerly known as Yucca Mountain Site Characterization Office (YMSCO), the participants in Task 2B/2C are ENRESA of Spain, CEA of France and the NRC of the United States. The research team of ENRESA is led by Prof. Sebastia Olivella of the UPC in Barcelona, Spain. Sui-Min Hsiung of the Center for Nuclear Waste Regulatory Analyses of the Southwest Research Institute in San Antonio, Texas leads the NRC's Task 2C research team. Alain Millard is the leader of CEA's Task 2C research team. The DOE's research teams are led by Robin N. Datta.

3. Comparison of results and overall evaluation

The four research teams, namely UPC (for ENRESA), CEA, LBNL (for DOE), and CNWRA (for NRC) prepared reports on the outcome of each team's research on Task 2B/2C. These reports are enclosed herewith in Attachments A (Olivella et al., 2004), B (Millard, 2004), C (Rutqvist, 2004) and D (Hsiung and Chodhury, 2004), respectively. A discussion of the results of the research follows.

The Yucca Mountain Drift Scale Test (DST) is a multiyear, large-scale underground heating test within the US Department of Energy's program for the site characterization at Yucca Mountain, Nevada. The test is designed to study coupled thermal-hydrological-mechanical-chemical (THMC) behavior in unsaturated fractured and welded tuff. As part of the international cooperative project DECOVALEX III (DEvelopment of COupled models and their VALidation against EXperiments, project phase III), four research teams used four different numerical models to simulate and predict coupled thermal-hydrological-mechanical (THM) processes at the DST. The simulated THM processes included (above boiling) temperature changes, liquid and vapor water movements, rock stress and displacements, and THM-induced changes in fracture permeability. The predicted THM responses were compared to *in situ* measurements of temperature, water saturation (estimated through geophysical measurements), rock-mass displacements, and changes in air permeability.

The codes and basic approaches used by the four research teams within the DECOVALEX III project follows. The LBNL and UPC teams performed coupled THM analyses that included modeling of two-phase fluid flow (air and water), heat transfer (conduction and convection), and mechanical stress and strain. LBNL used a dual-permeability (DKM) approach for simulation of TH processes, whereas UPC used an equivalent continuum model. CEA and CNWRA did not simulate fluid flow and heat transfer, but performed TM analyses in which the measured temperature field was imported to the numerical models. The measured temperature from the several thousand sensors in the DST test block was interpolated into a three-dimensional temperature field, which in turn was interpolated to nodal points in the numerical mesh of the CEA and CNWRA models. For simulation of rock-mechanical behavior, LBNL and UPC used elastic models, whereas CEA and CNWRA applied various elasto-plastic models. TM-induced permeability changes were modeled by three of the four teams: LBNL, UPC, and CNWRA. LBNL and CNWRA correlated permeability to fracture aperture in orthogonal fracture sets, where the fracture aperture is controlled by fracture normal stress. UPC correlated permeability to porosity, where porosity is controlled by volumetric strain.

In general, all teams discretized the DST test area into two-dimensional vertical cross sections through the center of the heated drift. A two-dimensional geometry was deemed sufficient for predicting TM-induced rock displacements and permeability changes at selected monitoring boreholes in the vertical x-z plane. However, the temperature in the heated drift may be overestimated in a two-dimensional model as a result of *in situ* three-dimensional out-of plane heat loss and because of heat loss through a bulkhead at the entrance of the heated drift. UPC therefore reduced the heater power applied in its simulation to be 70% of the actual heat power. LBNL did not reduce the simulated heat power, but found a good agreement with the measured temperature if loss of heat and vapor through the bulkhead was explicitly simulated. To simulate the bulkhead, LBNL added an extra grid element with properties

corresponding to a heat-loss coefficient of 0.4375 W/°K, determined through model calibration against early temperature data.

Model dimensions, boundary and initial conditions were assigned by each individual team based on site information. The lateral and vertical dimensions of the models used by each team vary from a few hundred to thousand meters. However, considering the limited extent of the heated rock volume during the four-year heating period, the boundaries of all four models are judged to be sufficiently far away from the drift to avoid adverse boundary effects on the simulated near field THM responses. The initial stress field varies somewhat among the research teams. In general at Yucca Mountain, the maximum principal stress is vertical, with its magnitude approximated by the weight of the overburden rock mass. Considering the depth of the DST, ground surface topography, densities of the overlying rock units, the vertical stress should be in the interval 4 to 6 MPa. The horizontal stresses are more uncertain because only a limited number of stress measurements have been conducted in the Tptpmn rock unit. The horizontal stresses at Yucca Mountain have been estimated to be about half of the vertical, but the ratio of horizontal to vertical stress could vary between 0.3 to 1.0. Recent stress measurements around the ESF confirm that horizontal stresses are lower than the vertical and indicates a minimum horizontal stress around 2 MPa and maximum horizontal stress of about 2.5 to 4 MPa. Because the thermal and mechanical responses at the DST are caused by thermally induced stresses, which are independent of the initial stresses, the initial stress may have little effect on the simulation results. However, the magnitude of initial horizontal stress affects the potential for developing tensile failure and shear slip in regions of thermal stress relief away from the heated drift.

The individual research teams derived material properties suitable for their respective modeling approach using site data from Yucca Mountain project reports. The hydrologic properties used by LBNL include water-retention and relative-permeability functions representing fractured and matrix continua, whereas UPC uses equivalent continuum properties representing a composite effect of matrix and fractures. The rock-mechanical properties include rock-mass deformability and strength. The Young's modulus adopted for the fractured rock mass by LBNL and CNWRA is about 50% of the values of intact rock, whereas UPC and CEA used intact-rock values. Strength properties used in the elasto-plastic ubiquitous joint models used by CEA and CNWRA are comparable. However, the two most important parameters for simulation of THM responses at the DST are coefficient of thermal expansion and a function defining the relationship between fracture normal stress and permeability. LBNL, CNWRA, and CEA adopted temperature dependent thermal expansion coefficients representing values determined from intact core samples. UPC used a constant value, which on the average is about twice the thermal expansion adopted by the other teams.

The permeability changes at the DST were predicted by LBNL, CNWRA, and UPC, using individually derived stress-versus-permeability functions. LBNL derived a stress-versus-permeability function based on a conceptual model of highly fractured rock containing three orthogonal fracture sets.

CNWRA used a similar approach to that of LBNL, but the model contains only two orthogonal fracture sets (see schematic of fractured rock model for CNWRA in Fig. 4). A deformation-permeability relationship based on the Bandis hyperbolic fracture normal closure model was extended to include corrections for shear dilation. UPC applied an empirical permeability-versus-porosity relationship.

The main difference between the three stress-versus-permeability models are that LBNL and CNWRA calculate changes in permeability based on the normal stress for a number of orthogonal fracture sets, whereas UPC calculates changes in permeability

based on changes in mean stress. Thus, changes calculated by LBNL and CNWRA can be anisotropic, depending on normal stress across different fracture sets, whereas UPC calculates isotropic changes in permeability controlled by changes in mean stress. Fig. 4 compares the stress-permeability-functions of the three research teams, for a special case of isotropic changes in stress. For an isotropic stress change, the various functions show some similarity, although there are differences in slope and residual permeability.

Comparing simulated and measured rock temperatures is a first step in evaluating the models since temperature change is the driving force behind the coupled THM processes at the DST. Comparisons of simulated and measured displacements and changes in air permeability allow further insights to be gained into model performance.

There are reasonably excellent agreement between simulated and measured temperature for LBNL's modeling and a reasonably good agreement for UPC's modeling. The difference in simulated temperature between LBNL and UPC can be explained by their respective approaches of simulating out of plane and bulkhead heat loss. UPC reduced the heat power input to their two-dimensional model simulation to about 70% of the actual heat power. Although this approach results in an overall reasonable agreement with measured temperature, it overestimates the heat loss during the first year and underestimates the heat loss towards the end of the heating period. The excellent agreement achieved by LBNL between simulated and measured temperature throughout the four-year heating period shows that the explicit simulation of the bulkhead with an additional element provides an accurate representation of heat loss. It correctly simulates heat loss as being proportional to the thermal gradient across the bulkhead, rather than being proportional to the heating power. CEA and CNWRA research teams did not perform a temperature simulation, but imported the measured temperature into their models.

The research teams were asked to predict the time evolution of rock-mass incremental displacements along extensometer boreholes for a borehole array located at $y = 21$ m (i.e. close to the middle of the axial extension of the drift). Sensitivity analyses showed that displacement magnitudes are mainly dependent on the coefficient of thermal expansion, whereas the elastic modulus of the rock has a smaller impact. The thermal expansion coefficient adopted by LBNL, CEA, and CNWRA are similar with intact-rock values determined on core samples. The UPC team used a thermal expansion coefficient that on average was twice the value of any other team and consequently calculated displacement values about twice as large. Because the thermal expansion coefficient adopted by the UPC team is twice as high as any other team (and twice as high as the thermal expansion of intact rock), an intercomparison is not meaningful, and therefore, UPC's displacement results are excluded in the discussion below.

In general, the displacements predicted by LBNL, CEA, and CNWRA are consistent for elastic models, with larger incremental displacement for anchors located farther away from the drift wall. Using elastic mechanical models, the simulated displacements along borehole 155 are very close to these measured for anchors 3 and 4, whereas the displacement for anchors 1 and 2 is underpredicted. The CEA's elasto-plastic ubiquitous joint model overpredicts displacements, especially in anchors 3 and 4. The results for borehole 156 shows excellent predictions of displacement in anchor 3, whereas the displacements in anchors 2 and 4 are generally underpredicted. Most notably, the CEA's elasto-plastic ubiquitous joint model provides the best prediction for anchor 4 of borehole 156, both in trends and magnitude.

The research teams were asked to predict the evolution of fracture permeability at specific borehole locations where air-injection tests are conducted at regular time intervals of about three months. In this paper, three borehole sections—denoted 76:4, 74:4 and 76:1, located in a borehole array at $y = 30.2$ m—are selected for a detailed

comparison of simulated and measured evolution of fracture permeability. These borehole sections were selected for comparison because they represent characteristic responses of fracture permeability at various locations around the heated drift: near the heat source (Section 76:4), far above the heat source (Section 74:4), and far on the side of the heat source (Section 76:1).

Changes in air permeability are caused by the combined effect of TH-induced changes in fracture moisture content and TM-induced changes in fracture aperture. TH-induced changes in fracture moisture content cannot be observed by direct measurements, since the moisture in the fracture system is only a small fraction of the total moisture content of the fracture-matrix system. However, the extent of the dryout zone at the DST is estimated by geophysical methods that include ground penetrating radar, electric resistivity tomography, and neutron log. A comparison of those geophysical data with the results by LBNL and UPC indicates that the extent of the dryout zone is controlled by the boiling temperature isotherm, and is well captured in the numerical results. TM-induced changes in fracture permeability are controlled by thermal stress and the adopted stress-versus-permeability relationship. The calculated thermal stress is in turn a function of calculated temperature changes, the thermal expansion coefficient, and the modulus of rock-mass deformation. A direct comparison of the thermal stresses calculated by different teams was not performed. However, based on the thermal expansion coefficient and Young's modulus adopted by each team, the thermal stress should be roughly a factor of four higher for UPC compared to LBNL and CNWRA. Such difference in the calculated thermal stress impacts the time evolution of TM-induced changes in fracture permeability.

Sensitivity studies by LBNL, UPC, and CNWRA show that the stress-versus-permeability relationship is the most important parameter for predicting the evolution of the fracture permeability. Obviously, if a more sensitive relationship between stress and permeability is adopted in the analysis, stronger changes in permeability will be predicted. It was also shown by LBNL and CNWRA that the permeability changes in vertical and horizontal fractures could be very different in some areas around the drift. In general, though, the permeability changes more in vertical fractures than in horizontal one, because vertical fractures are exposed to greater TM-induced stress changes.

At Section 76:4, the three teams correctly predict a decrease in air permeability during the first two years. This decrease in air permeability is the combined effect of TM-induced fracture closure and TH-induced condensation in the fracture system. The analyses by LBNL and CNWRA show that TM-induced decrease in intrinsic permeability occurs both in vertical and horizontal fractures. Therefore, the measured decrease is also well captured using the mean stress based model by UPC. After about two years of heating, the measured air permeability appears to recover somewhat. LBNL and UPC capture this partial recovery of air permeability as a result of drying of the fracture system. CNWRA, on the other hand, does not capture such recovery because they did not account for TH-induced changes in moisture content within their analysis.

At section 76:1, LBNL and UPC predict a slow gradual reduction in air-permeability with time. CNWRA predicted a slight increase during the first year, and thereafter a slight fluctuation between 1 and 1.2, until the end of the heating. The simulated results are roughly similar to the measured, with better agreement achieved by LBNL and UPC. The analyses by CNWRA and LBNL showed that at this location the intrinsic permeability of vertical fractures decreases, while the intrinsic permeability of horizontal fractures slightly increases. In the field, the net effect is a slight decrease in air permeability.

For Section 74:4, measured air permeability increases during the first two years and then gradually decreases. Only LBNL appeared to be able to correctly simulate the magnitude of the increasing permeability during the first two years. The LBNL and CNWRA analyses showed that at 74:4, an increasing permeability can be explained by a reduction in horizontal stress that tends to increase the aperture of vertical fractures. In LBNL's simulation, the increasing permeability of the vertical fractures is sufficiently large to induce a net increase in mean permeability. In CNWRA's simulation, on the other hand, increasing permeability in the vertical fractures was completely offset by a decreasing permeability in horizontal fractures.

The generally good agreement between simulated and measured temperature, displacement, and changes in air permeability shows that the numerical models and underlying conceptual models are adequate for simulating coupled THM processes at the DST. From the analyses and discussions presented, the following specific conclusions can be drawn:

- ❑ A continuum model approach is adequate for simulating relevant coupled THM processes at the DST.
- ❑ TM-induced rock deformations are generally well simulated using an elastic model, although some individual displacements appear to be captured using an elasto-plastic model.
- ❑ The highest potential for inelastic deformation in the form of fracture shear slip occurs near the drift wall and in a zone of thermal stress decrease located more than 15 m above the heated drift.
- ❑ Despite potential shear slip along fractures, fracture closure/opening caused by change in normal stress across fractures is the dominant mechanism for TM-induced changes in intrinsic fracture permeability, whereas fracture shear dilation appears to be less significant at the DST.

The last conclusion, made from the analysis of the heating phase at the DST, indicates that TM-induced changes in permeability at the DST, which are within one order of magnitude, tend to be reversible.

References

- CRWMS M&O. *Drift Scale Test As-Built Report*. B000000000–01717–5700–00003. Rev. 01. Las Vegas, Nevada: CRWMS M&O. 1998.
- CRWMS M&O. *Drift Scale Test Design and Forecast Results*. BAB000000–01717–4600–00007. Rev. 01. Las Vegas, Nevada: CRWMS M&O. 1997.
- Hsiung S. M. and Chowdhury A. H. *Final report for DRCOVALEX III task 2C: Thermal-mechanical modeling of the drift-scale heater test at yucca mountain*. 2004.
- Milar A. *THM modeling of DST insitu test at Yucca Mountain*. Final report for DECOVALEX III Task 2C. 2004.
- Olivella S., Gens S. and Ganzalez C. *THM modeling of DST insitu test at Yucca Mountain*. Final report for DECOVALEX III Task 2B. 2004.
- Rutqvist J. *TOUGH-FLAC Coupled Thermal-hydrological-mechanical Analysis of the Yucca Mountain Drift Scale Test within the Framework of the DECOVALEX III Project*. Final report for DECOVALEX III Task 2B. 2004.